ELSEVIER

Bone Vol. 26, No. 3
March 2000:207–213

RAPID COMMUNICATION

The Gene Encoding the Mouse Homologue of the Human Osteoclast-Specific 116-kDa V-ATPase Subunit Bears a Deletion in Osteosclerotic (*oc/oc*) Mutants

J.-C. SCIMECA,[1] A. FRANCHI,[1] C. TROJANI,[1] H. PARRINELLO,[1] J. GROSGEORGE,[1] C. ROBERT,[2] O. JAILLON,[2] C. POIRIER,[3] P. GAUDRAY,[1] and G. F. CARLE[1]

[1]*Instabilité et Altérations des Génomes, UMR6549 CNRS/UNSA, Faculté de Médecine de l'Université de Nice-Sophia Antipolis, Nice, France*
[2]*Génoscope, Centre National de Séquençage, Evry, France*
[3]*Unité de Génétique des Mammifères, Institut Pasteur, Paris, France*

Osteosclerosis (*oc*) is an autosomal recessive lethal mutation that impairs bone resorption by osteoclasts, and induces a general increase of bone density in affected mice. Genetic mapping of the *oc* mutation was used as a backbone in a positional cloning approach in the pericentromeric region of mouse chromosome 19. Perfect cosegregation of the osteopetrotic phenotype with polymorphic markers enabled the construction of a sequence-ready bacterial artificial chromosome (BAC) contig of this region. Genomic sequencing of a 200-kb area revealed the presence of the mouse homologue to the human gene encoding the osteoclast-specific 116-kDa subunit of the vacuolar proton pump. This gene was located recently on human 11q13, a genomic region conserved with proximal mouse chromosome 19. Sequencing of the 5′ end of the gene in *oc/oc* mice showed a 1.6-kb deletion, including the translation start site, which impairs genuine transcription of this subunit. The inactivation of this osteoclast-specific vacuolar proton ATPase subunit could be responsible for the lack of this enzyme in the apical membranes of osteoclast cells in *oc/oc* mice, thereby preventing the resorption function of these cells, which leads to the osteopetrotic phenotype. (Bone 26:207–213; 2000)

Key Words: Osteopetrosis; oc mutant; V-ATPase; Physical mapping; Mouse chromosome 19.

Introduction

Osteopetrosis, also known as marble bone disease, is a metabolic bone disorder that is characterized by a general increase of bone density resulting from a defect in osteoclast presence or function. Several genetically inherited forms of the disease have been described in humans. There are four spontaneous osteopetrotic mutations in mice that have been reported: *op/op* (osteopetrosis), *mi/mi* (microphtalmia), *gl/gl* (grey-lethal), and *oc/oc* (osteosclerosis). The osteoclast deficiency in *op/op* mice is due to a mutation in the coding region of the macrophage colony-stimulating factor gene (M-CSF1),[22] and a defect in a gene coding for a helix-loop-helix transcription factor is responsible for the microphtalmia phenotype.[13] Currently, the genes associated with *oc* or *gl* mutations have not been identified.

Osteosclerosis (*oc*) is a mouse osteopetrotic mutation inherited as an autosomal lethal recessive trait that arose spontaneously in 1966 at the Jackson Laboratory in the C57BL/6J-*bf* strain,[5] and has been backcrossed over 20 times to the hybrid C57BL/6Jle × C3HeB/FeJLe-*a/a* F_1, in order to increase the survival time of the affected *oc/oc* animals. The *oc/oc* homozygote mice usually die around 3 weeks of age, and the mutation has been maintained in *oc*/+ heterozygotes, which do not display any particular phenotype. Affected animals (*oc/oc*) exhibit the characteristic radiologic and histologic features of osteopetrosis, including a generalized increase in skeletal density and absence of marrow cavities easily detected by X-ray radiography (**Figure 1**).

Oc was originally mapped to mouse chromosome 19 (MMU19) with fairly loose precision by Lane.[14] In 1985, Marks et al.[17] gave a better characterization of the phenotype and anchored the mutation in the pericentromeric region of MMU19. However, in this initial genetic mapping effort, the closest phenotypic marker brachymorphic (*bm*) was located 30 cM telomeric of *oc*, and no close markers were shown to segregate with the osteopetrotic phenotype. We have undertaken a comparative mapping study of a syntenic area of the genome that has been conserved through evolution between human 11q13 and the pericentromeric region of mouse chromosome 19.[4,8,21] Many genes involved in inherited human pathologies and localized on 11q13 have an homologous gene present on proximal MMU19 region and vice versa.[20] This gene conservation between mice and humans has been very helpful in designing new probes to refine the physical map. Moreover, it has been a source of candidate genes for positional cloning in both species. In our attempt to identify candidate genes for *oc*, we were able to exclude the Fos-related antigen 1 gene (*fra-1*), based on its segregation pattern and an allelism test,[19] as well as a putative transporter gene (*Roct1*),[3] based on physical mapping results (data not shown).

The positional cloning approach we followed consisted of four phases: defining the smallest candidate region based on proximal and distal meiotic recombination events, constructing a high-density physical map, sequencing the region of interest, and performing genomic database comparisons. In this report, we

Address for correspondence and reprints: Dr. Georges F. Carle, Instabilité et Altérations des Génomes, UMR6549 CNRS/UNSA, Faculté de Médecine de l'Université de Nice-Sophia Antipolis, 06107 Nice, France. E-mail: carle@unice.fr

8756-3282/00/$20.00
PII S8756-3282(99)00278-1

Bone Vol. 26, No. 3
March 2000:207–213

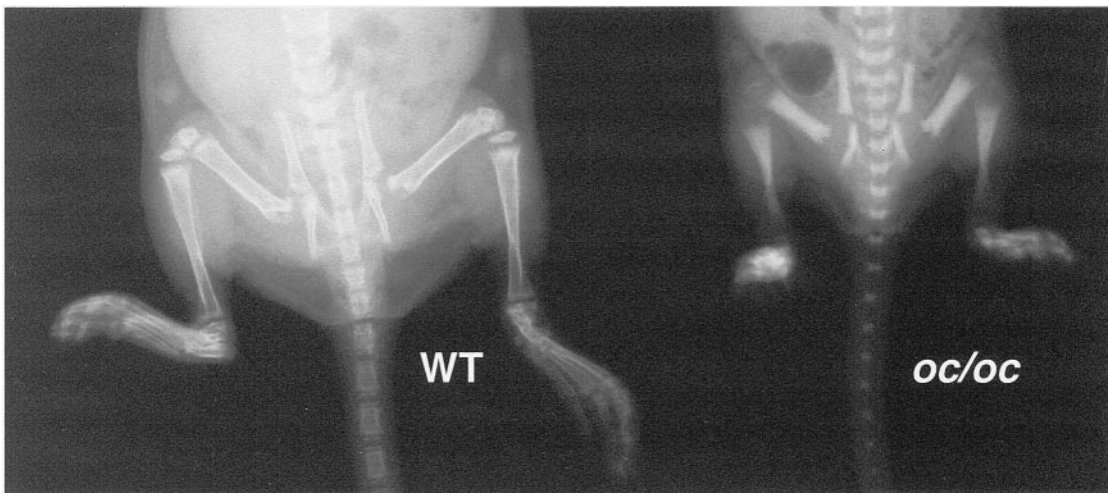

Figure 1. Radiographic images of a 14-day-old normal mouse (wt) and its osteosclerotic littermate (*oc/oc*). A general increase of bone density and disappearance of bone marrow space can be observed in the mutant.

present evidence showing a 1.6-kb genomic deletion in mouse osteosclerotic mutants (*oc/oc*) removing the translation start site in the gene homologous to the human OC 116-kDa osteoclast-specific vacuolar proton pump subunit.

Materials and Methods

Mice

Two pairs of (C57BL/6J × C3HheB/FeJ) F1 *oc*/+ mice were initially obtained from the Jackson Laboratory (Bar Harbor, ME) and maintained in our central animal facility in accordance with the general guidelines edicted by the Direction des Services Vétérinaires. Heterozygotes animals (*oc*/+) were identified 3 weeks after birth by DNA genotyping (tail clipping) with a polymorphic marker (*D19Mit68*) cosegrating with the mutation. Animals suspected to be homozygous at the *oc* locus (smaller size than littermate, circling behavior, absence of or delayed incisors eruption) were systematically submitted to radiographic analysis for final phenotyping. *Mus spretus* mice (SEG imbred strain) were obtained from the Unité de Génétique des Mammifères (Institut Pasteur, Paris).

Yeast Artificial Chromosome (YACs) and Bacterial Artificial Chromosome (BAC) Identification

We initially identified YACs from the candidate region by screening four different mouse libraries (Princeton Library, MIT/Whitehead Institute Library, St Mary's Hospital Library, and Imperial Cancer Research Fund (ICRF) Library). The screenings were performed with the help of either the Princeton or Généthon screening facility. BACs were then identified with polymerase chain reaction (PCR)-based screening of pooled libraries (Research Genetics, Huntsville, AL) with various STS from the interval. STS were obtained, mainly from BAC end-sequencing, but also by taking advantage of the conservation between HSA11q13 and the pericentomeric region of MMU19.

BAC DNA Purification and BAC End-Sequencing

BAC DNAs were prepared using a Nucleobond PC kit from Macherey-Nagel (Hoerdt, France), according to the manufacturer's instructions. BAC end-sequencing reactions were performed with 5 μg of template, using the Thermo Sequenase kit (Amersham, Les Ulis, France), and IRD700- or IRD800-labeled SP6 or T7 primers (MWG Biotech, Ebersberg, Germany). Sequencing reaction products were analyzed on a LI-COR Long ReadIR 4200 DNA sequencer (LI-COR Inc., Lincoln, NE)

Polymerase Chain Reaction

Polymerase chain reaction was performed using primers and annealing temperatures reported in **Table 1**. The 25-μL reaction volume contained 25 pmol of each primer, 3.13 pmol dNTPs, 1.5 mmol/L $MgCl_2$, and 0.5 U of platinium Taq DNA polymerase (Life Technologies, Cergy Pontoise, France). After 2 min at 95°C, PCR was carried out for 35 cycles with the following steps: 94°C for 30 sec, annealing temperature for 30 sec, and 72°C for 30 sec. A final extension step at 72°C for 10 min concluded each reaction. Amplification was performed in a PTC-100 thermal cycler (MJ Research, Waltham, MA). Polymerase chain reaction products were analyzed by gel electrophoresis in 2% agarose gels.

MMUOC116 Positioning on the Physical Map

We used two primer pairs (D19 Car333 and D19Car319) for the positioning of MMUOC116, as illustrated in **Figure 3**. Each pair corresponded, respectively, to the 5′ and to the 3′ end of the mouse gene, and upstream and downstream primers were as follows: D19Car333, 5′-TAGCTTGAAGCAGATTGTACG-3′ and 5′-CTCAACTTCGGCTTAGGATC-3′; D19Car319, 5′-CAGCTCTTTATTCCTGTCCC-3′ and 5′-CTTCATGCACCAAGCAATCC-3′.

FISH

BAC DNA was labeled using nick-translation with biotin-14-dATP (Life Technologies). The labeled probe (1 μg/slide) was coprecipitated with 30 μg of mouse Cot-1 DNA (Life Technologies), denatured for 5 min at 70°C in hybridization mixture (50% formamide, 2× SSC, 10% Dextran sulfate), and reannealed for 30–60 min at 37°C. The probe was then hybridized on denatured pretreated metaphase chromosomes from mouse SV22-CD cell line[2] overnight in a moist chamber at 37°C. The following steps were performed as described previously.[8]

Table 1. Primers for PCR amplification of physical and genetic mapping markers

Marker	Forward primer	Reverse primer	T_A (°C)	Product (bp)[b]	Reference
D19Car5[a]	5′-GCT GGC TTT AGA CTG ATT TG-3′	5′-GGG CTT CAT AGT GAG AC-3′	50	125	This study (YAC end)
D19Car10	5′-CTC CTG AAG ATG AGA AAT CTC C-3′	5′-GCT ACA TAG AAG ACC TTT GCC-3′	60	129	Fernandes et al., 1998
D19Car14 (Gstp1)	5′-GAT CTC CTT TGC CGA TTA CA-3′	5′-TTG CCA TTG CCA TTG ATG GG-3′	54	183	Bammler et al., 1994[c]
D19Car51	5′-GCC TCT CTG ATG ACA TAT AAT G-3′	5′-AGA GAA ACT GTT TTA CTT ACC AG-3′	60	140	This study (BAC end)
D19Car53	5′-CTG TCT GCG GCA GTG AGG-3′	5′-AGA CAC CAT CCA ACA CGT CA-3′	58	182	This study (BAC end)
D19Car55	5′-TTC ATC ACC TGT CAG ACA GG-3′	5′-GTG TCA ATC ATA AGG GCC AG-3′	58	248	This study (BAC end)
D19Car57	5′-TTA ATG CCA GCA CTT GGG GA-3′	5′-TAC AGA TGG TTT TGA GCC CC-3′	58	245	This study (BAC end)
D19Car61	5′-AGA ACG GTT TCC TTC ACA GC-3′	5′-TGT GTG TGA CTA CAA CTG GC-3′	58	435	This study (BAC end)
D19Car63	5′-CAT TAC CTC AGC TCA GTC TC-3′	5′-GGG ATG GGA ATA TGT CTC AG-3′	58	182	This study (BAC end)
D19Car71	5′-ATC AAC AAG TGG CCA CTG AG-3′	5′-GCA TCA ACA GCA GGA GCT G-3′	58	256	This study (BAC internal)
D19Car75	5′-AGC CTC CAA CTC CTA GAA ATC-3′	5′-CCC TGG AAC TGG TGT TAC AG-3′	60	233	This study (BAC internal)
D19Car77	5′-GTC TAC AGA GTG AGT TCC AG-3′	5′-ATC TGT CGG GAA ACC CTC C-3′	58	199	This study (BAC internal)
D19Car87[a]	5′-TAC TCT ATC CAC TGC ATG GG-3′	5′-TCC ATT CCT TCC ACA ACC TG-3′	58	303	This study (BAC end)
D19Car89	5′-ACT CAA GGA GGC TAA GAT GC-3′	5′-TCT CCT GAC CTC TAC AAA CG-3′	58	404	This study (BAC end)
D19Car235	5′-ACT ACA TAG CTG AGG GTG AC-3′	5′-CTG CTC TCC TCA GTT CAC G-3′	58	229	This study (BAC end)
D19Car237	5′-AGC TGT CTT GGA GCC TCA G-3′	5′-AGA CTA GAG CTT CTC TCT GG-3′	58	170	This study (BAC end)
D19Car239 (Smbp2)	5′-CAT CCA ATC GTG ATG ACA GC-3′	5′-GAT GAG TTG GAG ATG AAG CG-3′	58	234	Mizuta et al., 1993[d]
D19Car241	5′-TGG AGA GAG GAT TCG GCT G-3′	5′-CAA TGA CTG TGA CTT CAA CTC-3′	58	113	GenBank AA209103
D19Car243[a]	5′-AGC TGG CCT TTG ATT ATG TAG-3′	5′-TAT ACT CTC ATA TGT GGC AGC-3′	58	136	This study (BAC internal)
D19Car245[a]	5′-TAT GGA CAC ACT GTG CGC G-3′	5′-AAG TGC TAG GAT TTG AGA GAC-3′	58	149	This study (BAC internal)
D19Car247[a]	5′-CTA GCC TGC CTA GAC AAC C-3′	5′-GCA GAG AAG TGA ATG CTA GG-3′	58	147	This study (BAC internal)
D19Car285	5′-GGT CTC TCT TGG ATA ACT CC-3′	5′-CTA ATC TTC ACT GGC TCA CC-3′	58	180	This study (BAC end)
D19Car295 (Galn)	5′-GTG CAG TAA GCG ACC ATC C-3′	5′-TGG CTG ACA GGG TCA CAA C-3′	58	363	Kofler et al., 1996[e]
D19Car301	5′-AAC ATG CTT GGC TGT AGG C-3′	5′-CAG CCT ACA GAG TGA GAC C-3′	58	199	This study (BAC end)
D19Car303	5′-CCC TGT TGA CTT CTT TCT GG-3′	5′-ACC ATG TAT GCC AGG CTG G-3′	58	258	This study (BAC end)
D19Car307	5′-GCC ATA AGA GAC CCA GAG C-3′	5′-GGT GGT GAA TCA GAT GTT GG-3′	58	180	This study (BAC end)
D19Mit32[a]	5′-GGT GCA CAT GTG TAC ATG CA-3′	5′-TGC AGA ACC TGC TGT ATG TTG-3′	58	152	MGI:91242
D19Mit68	5′-CCA ATA CAA ATC AGA CTC AAT AGT CG-3′	5′-AGG GTC TCC CCA TCT TCC TA-3′	60	136	MGI:91281
D19Mit93[a]	5′-CCT GGC CTC ACC TTT TTA CA-3′	5′-ACA TGC GCT GTG GCT CTC-3′	56	114	MGI:100754

[a]PCR assays generating a polymorphic product (C57BL/6 ≠ *Mus spretus*).
[b]C57BL/6 alleles.
[c]Biochem J 298:385–390, 1994.
[d]Nucl Acids Res 21: 1761–1766, 1993.
[e]Gene 182: 71–75; 1996.

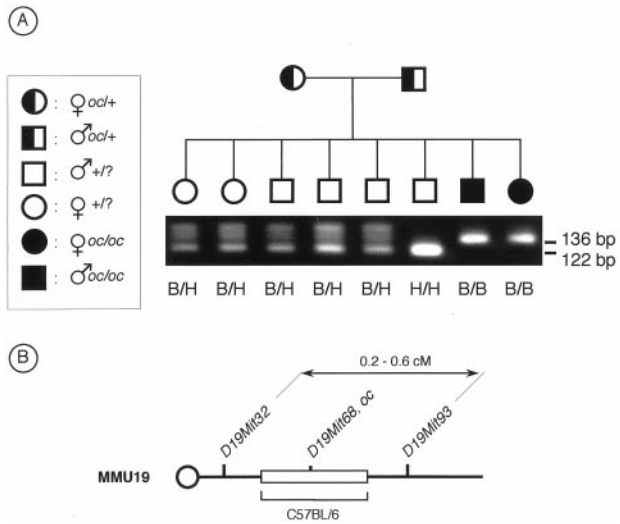

Figure 2. (A) Genotyping of an *oc*/+ × *oc*/+ cross with the polymorphic microsatellite *D19Mit68*. Mutant *oc/oc* mice show the cosegregation of the osteopetrotic phenotype with C57BL/6 alleles (B/B). (B) Schematic representation of the C57BL/6 minimal region cosegregating with *D19Mit68* and the *oc* locus. Recombinant *oc/oc* and *oc*/+ animals excluded *D19Mit32* and *D19Mit93* as proximal and distal boundaries, respectively. The genetic distance between these two boundaries is derived from the EUCIB data.

BAC Sequencing and Clone Assembly

BAC DNA was prepared according to a standard alkaline lysis protocol, and purified twice on a CsCl gradient. BAC DNA (20 μg) was mechanically disrupted using a hydroshear device (Gene Machines, San Carlos, CA), generating genomic DNA fragments an average of 3 kb in size. BAC DNA fragments were repaired with T4 DNA polymerase, and ligated to BstXI adaptors (Invitrogen, Groningen, The Netherlands). DNA adaptor-ligated fragments were purified by electrophoresis on a 0.7% agarose (FMC Bioproducts, Rockland, ME) preparative gel. After electrophoresis, fragments were excised from the gel, purified on Qiaquick columns (Qiagen, Courtaboef, France), and ligated to pcDNA2.1 vector (Invitrogen). Recombinant plasmids were transformed into *Escherichia coli* DH10B cells by electroporation (Electromax; Life Technologies). Ampicillin-resistant bacterial clones were picked with a Flexy robot (Proteigene, Saint-Marcel, France) and inoculated in 96-well arrays. Clones corresponding to 12 96-well dishes (8× BAC length) were end-sequenced on a Licor 4200 system (Li-Cor Inc., Lincoln, NE). Sequence assembly was performed using the Phred-Phrap software.[7]

Genomic DNA Amplification and Sequencing

Genomic DNA (50–100 ng) (prepared from mouse tail) was used as a matrix for amplification with the following upstream and downstream primers: 5′-ATCCTAAGCCGAAGTTGAGC-3′ and 5′-TCCGTTTCCTCCTGGATGC-3′. Polymerase chain reaction products were purified using the High Pure PCR product purification kit (Roche Diagnostics, Meylan, France). After sequencing with IRD700-labeled reverse primer (MWG Biotech, Ebersberg, Germany), the analysis was performed as described above.

Reverse Transcription (RT)-PCR

We extracted total RNA from kidney with Extract All reagent (Eurobio, Les Ulis, France), and cDNA was generated using Expand reverse transcriptase (Roche) and $p(dT)_{15}$ oligonucleotide (Roche) in a 40-μL reaction volume under conditions recommended by the manufacturer. Polymerase chain reaction was performed with the following upstream and downstream primers: 5′-ATCCTAAGCCGAAGTTGAGC-3′ and 5′-TCCGTTTCCTCCTGGATGC-3′. Polymerase chain reaction products were purified using the High Pure PCR product purification kit, and subcloned into pGEMT-Easy vector (Promega) according to the manufacturer's protocol. Recombinant plasmids were transformed into JM109 competent bacteria. Plasmid DNAs were prepared using the Wizard Plus SV miniprep kit (Promega, Charbonnieres, France), digested with Not I (two sites flanking the cloning site of the vector), and analyzed by gel electrophoresis in 2% agarose gel. After sequencing of plasmid DNAs with IRD700-labeled SP6 and M13u (universal) primers (MWG), the analysis was performed as described above. The GenBank accession number is AF188702.

Results

Genetic Mapping of the oc Mutation

In the present study, we have been able to refine the genetic localization of the *oc* gene in the pericentromeric region of mouse chromosome 19 using an interspecific intercross of the type: (B6C3-*a/a* F1 *oc*/+ × *Mus spretus*)F1*oc*/+ × (B6C3-*a/a* F1 *oc*/+ × *Mus spretus*)F1*oc*/+. Close to 400 F2 progeny were generated, and using eight microsatellite markers (*D19Mit22*, *D19Mit31*, *D19Mit32*, *D19Mit42*, *D19Mit51*, *D19Mit68*, *D19Mit93*, and *D19Mit109*), polymorphic between C57BL/6, C3H, and *Mus spretus*, 24 +/? recombinants and 20 *oc/oc* recombinant animals were typed in more details (data not shown). Backcrossing the original mutant stock to B6C3-*a/a* F1 hybrids[17] in order to generate vigourous breeding stock introduced a C3H genetic background that was detected on MMU19 in heterozygotes *oc*/+ mice.

The analysis of these recombinants led to the definition of a minimal candidate region, with *D19Mit32* representing the centromeric boundary and *D19Mit93* the telomeric one. High-resolution genetic maps of mouse chromosomes have been generated in the European Collaborative Interspecific Mouse Backcross (EUCIB) project based on close to a thousand progeny produced by an interspecific backcross between C57BL/6 and *Mus spretus*.[6] In that project, the genetic distance between *D19Mit32* and *D19Mit93* ranges from 0.2 to 0.6 cM in the BSS and BSB crosses, respectively (http://www.informatics.jax.org/menus/map_menu.shtml).

Finally, the systematic genotyping of over 200 *oc/oc* mice generated from the (B6C3-*a/a* F1 *oc*/+) × (B6C3-*a/a* F1 *oc*/+) cross showed, invariably, B/B homozygous alleles for *D19Mit68* segregating with the osteopetrotic phenotype (an example of the pedigree is shown in **Figure 2**). Thus, a defined region bearing the C57BL/6 background in which the *oc* mutation appeared could be delimited by *D19Mit32* and *D19Mit93* and centered on *D19Mit68*.

Physical Mapping of the Candidate Region

Based on our genetic mapping results, a screening of YAC and BAC libraries was undertaken. From a first set of two YACs and three BACs, end probes were isolated and sequenced in order to derive new STS markers and build up a set of overlapping clones.

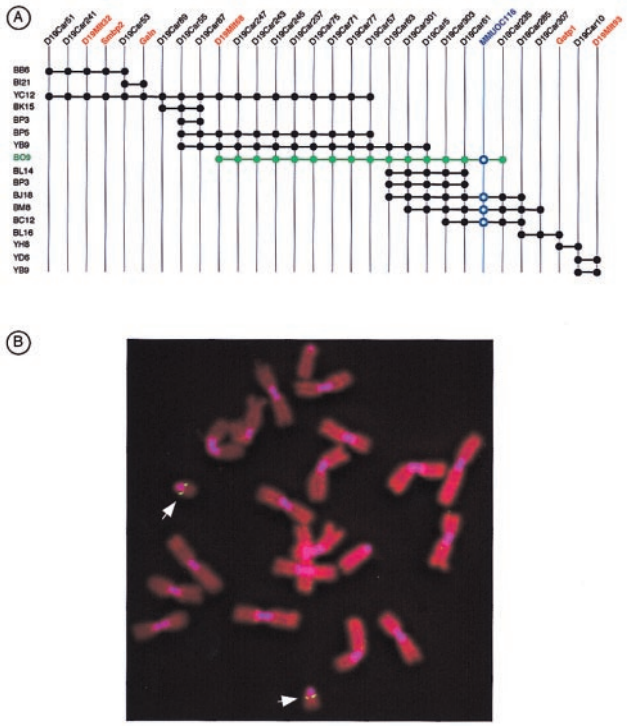

Figure 3. (A) BAC and YAC STS-based content contig map of the candidate region for the *oc* locus. Bxx and Yxx represent BAC and YAC references, respectively. Positive PCR assays with each genomic clone are represented by a dot. Open circles identify PCR assays corresponding to MMUOC116. (B) FISH hybridization on SV22CD mouse metaphase chromosomes using the BO9 BAC DNA as a probe.

A more in-depth study of the physical map of this region of the mouse genome will be published separately (manuscript in preparation). Five YACs and 12 BACs were finally retained for further characterization and were assembled in an STS content-based contig shown in Figure 3A. To ascertain the localization of the YAC and BAC genomic clones at the same time as testing for chimerism, fluorescent in situ hybridization was systematically performed on mouse SV22-CD metaphase chromosomes; an example of such hybridization using BAC BO9 DNA as a probe is shown in Figure 3B. Aside from the three microsatellite MIT markers, *D19Mit32*, *D19Mit68*, and *D19Mit93*, three genes conserved between HSA11q13 and MMU19 were positioned on this contig (*Gstp1*, *Smbp2*, and *Galn*). Twenty-one new STSs were generated from sequence data obtained either from BAC/YAC clone insert-end or internal sequencing. Oligonucleotide sequences for these PCR assays as well as the annealing temperature and the size of the product generated from a C57BL/6 DNA template are presented in Table 1. Five of these new STSs, present on BACs BP5 and/or BO9, display polymorphic PCR products between C57BL/6 and *Mus spretus*, which appeared to cosegregate with *oc/oc* animals like *D19Mit68* (data not shown). We then generated a 1.1-Mb contig based on a set of overlapping BAC/YAC clones including both proximal and distal boundaries of the candidate region where *oc* had been located.

A Mouse Homologue of the Human 116-kDa V-ATPase Subunit Gene (MMUOC116) Is Mutated in oc/oc Mice

The physical and genetic mapping results guided our choice in the selection of two BACs of 120 kb (BP5) and 220 kb (BO9) for shotgun cloning and sequencing. Sequence comparison using BLAST-based software[1] between one of the contigs of BAC BO9 against several database (nr GenBank, dbEST, dbSTS, . . .) identified five mouse ESTs (GenBank Accession Nos. AI663350, AI549720, AI180721, AI649394, AI607442) displaying sequence identity with one sequence contig of the BO9 clone. This set of ESTs showed a high degree of similarity to the cDNA sequence of a new human osteoclast-specific 116-kDa vacuolar proton pump subunit (OC-116KDa) (Genbank Accession No. U45285).[15] Based on the sequence of these five mouse ESTs, we

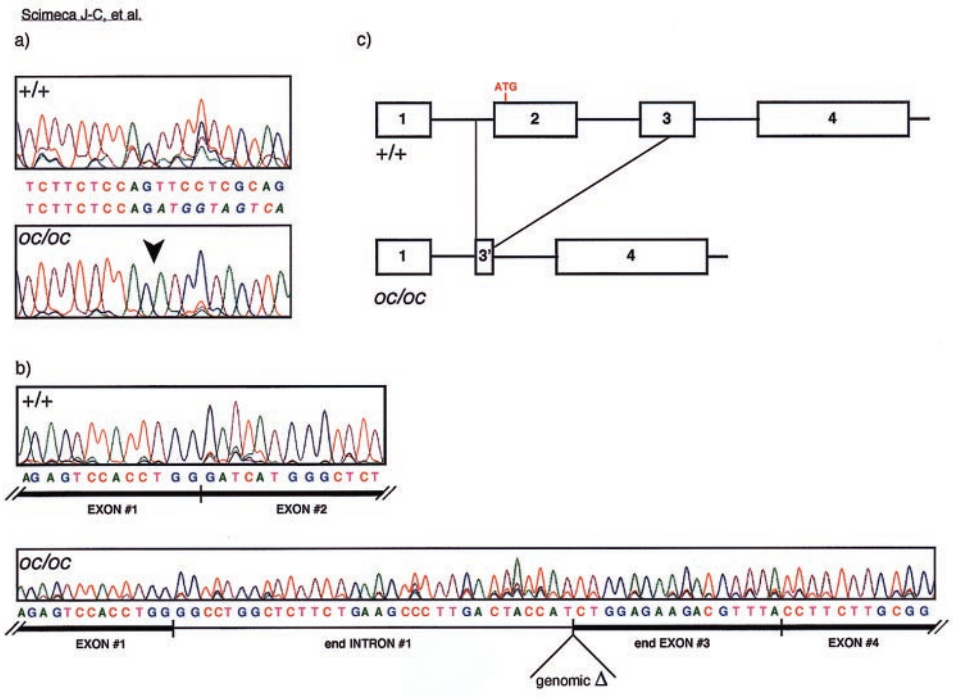

Figure 4. DNA sequence comparison of mouse OC116 gene in wt and in *oc/oc* mice. (a) The distal border of the deletion (exon 3 into intron1) in normal (+/+) and mutant (*oc/oc*) genomic DNA. (b) The expected exon 1/exon 2 junction in +/+ mice cDNA, and one of the alternative RT-PCR products derived from *oc/oc* mice. (c) A schematic representation of the 1.6-kb deletion in genomic DNA present in *oc/oc* mutants compared with the wild type.

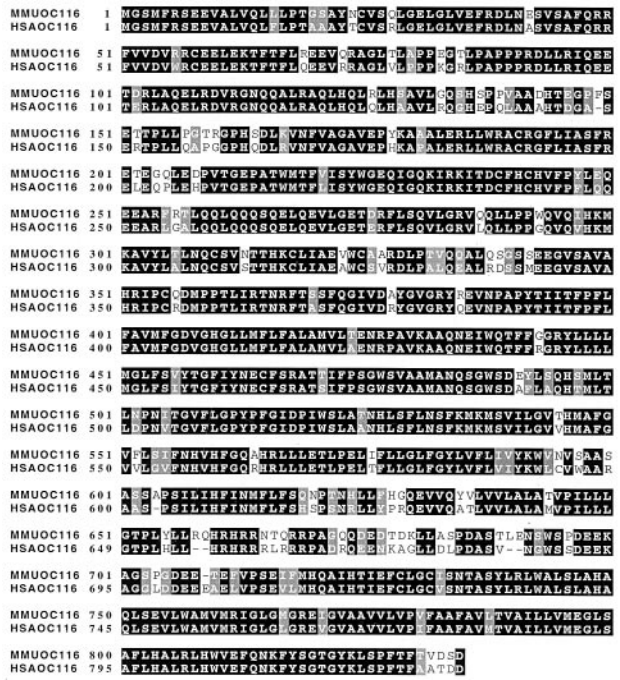

Figure 5. Amino acid comparison of mouse vs. human OC116 predicted protein sequences. Black boxes represent identical residues, while grey boxes correspond to similar ones.

designed oligonucleotide primers to perform RT-PCR experiments on mRNAs derived from kidneys of wt and *oc/oc* mice.

A set of primers chosen between exon 1 and exon 4 of OC116 revealed a major size difference between the RT-PCR products generated from wt or mutant mice (data not shown). While the corresponding bands of these RT-PCR products were gel purified, cloned, and sequenced, genomic sequencing was performed on DNA extracted from wt and *oc/oc* mice. A 1579-bp deletion starting in the middle of intron 1 and extending 62 bp into exon 3 was identified in the genomic DNA of *oc/oc* mice (**Figure 4**a,c). This deletion removes the translation start site present at the beginning of exon 2. The sequence analysis of RT-PCR products derived from *oc/oc* mice showed either exon 1/exon 4 junctions (data not shown) or an alternative splice site in intron 1, 32 bp upstream from the 1579-bp genomic deletion (Figure 4b). Thus, while RT-PCR products between exon 1 and 4 are accurately spliced in kidneys of wt mice, a large genomic deletion removing exon 2 and most of exon 3 results in aberrant mRNA transcripts in mutant animals.

The predicted protein encoded by the mouse homologue of OC116 displays 84% identities and 91% similitudes at the amino acid level with its human homologue (**Figure 5**). A recent study by Heinemann et al.[12] localized the OC116 gene at 11q13 by fluorescent in situ hybridization on human metaphase chromosomes and described the genomic organization of this gene. Based on these results and the sequence data of the five mouse ESTs described previously, we were able to predict the intron/exon structure of MMUOC116. Similarly to what was found by Heinemann et al., we identified 20 exons ranging from 79 bp (exons 1 and 3) up to 221 bp (exon 4). The translation start site is also present in exon 2, and the UAG stop codon is in exon 20. Thus, based on the MMUOC116 gene location and the high similarity of amino acid sequence with human OC116-predicted protein, it is very likely that the gene we isolated, as being mutated in *oc/oc* mice, is the mouse homologue of the human OC116 gene.

Discussion

We have isolated the mouse homologue of a new human osteoclast-specific vacuolar proton pump subunit gene that appears to be deleted over 1.6 kb at its 5′ end in osteosclerosis (*oc/oc*) mutants. This result was achieved by a positional cloning strategy starting from the segregation of the *oc* mutation in an interspecific genetic cross to define proximal and distal recombination boundaries, followed by physical mapping over several hundreds of kilobases, and finishing by the sequence of a 200-kb genomic area.

The human OC116 gene was isolated by Li et al. and reported as putative novel human osteoclast-specific vacuolar proton pump subunit.[15] We hypothesize that the 1.6-kb deletion present in *oc/oc* mice inactivates the normal expression of the MMUOC116 gene and, consequently, could be deleterious for the vacuolar proton pump localization and expression on apical membranes of osteoclast cells. Indeed, previous work by Nakamura et al.[18] demonstrated that although the vacuolar H^+-ATPase proton pump was still active in *oc/oc* mice and present throughout the cytoplasm, it was no longer found on the osteoclast apical membranes. One of the features of *oc/oc* mice osteoclasts is the absence of ruffled border formation, leading to a defect in bone resorption. Whether the mislocalization of the vacuolar proton pump to the outer membrane of osteoclasts is a cause or a consequence of this lack of ruffling remains to be discovered.

Recently, Heaney et al. described the mapping of human autosomal recessive osteopetrosis to a 14-cM interval on 11q13.[11] This rare form of human osteopetrosis is lethal within the first decade in the absence of bone marrow transplantation,[9,10] and its phenotype presents many similarities with the osteosclerosis mutation. Based on the present work, it is very likely that mutations affecting OC116 gene expression could be responsible for this form of human osteopetrosis. Sequencing of the entire OC116 genomic sequence of such affected individuals is presently in progress in our laboratory.

Finally, Li et al have recently presented an abstract at the 21st American Society for Bone and Mineral Research Meeting, showing that knockout −/− mice for the OC116 gene were growth retarded, developed severe osteopetrosis with deficiencies in bone remodeling and tooth eruption, and died at about 4 weeks of age.[16] All these phenotypic features are highly similar to what has been described for *oc/oc* mice, and strongly suggest that the genomic DNA deletion we observed in the MMUOC116 gene is sufficient to account for this phenotype.

Acknowledgments: The authors thank Jean-Marc Gaillochon, Gilles Gaudray, Jean-Noël Charrier, and José Barbe for technical assitance; and are very grateful to Philip Avner, Jean-Louis Guénet, and Jean Weissenbach for their support. This work was funded by grants from the Ministère de la Recherche (GREG N°59/94), the Association pour la Recherche contre le Cancer, and the GIP-Hoechst Marion Roussel (#FR/98BON005).

References

1. Altschul, S. F., Madden, T. L., Schaffer, A. A., Zhang, J., Zhang, Z., Miller, W., and Lipman, D. J. Gapped BLAST and PSI-BLAST: a new generation of protein database search programs. Nucleic Acids Res 25:3389–3402; 1997.
2. Baron, B., Metezeau, P., Kelly, F., Bernheim, A., Berger, R., Guenet, J. L., and Goldberg, M. E. Flow cytometry isolation and improved visualization of sorted

mouse chromosomes. Purification of chromosomes X and ISO-1 from cell lines with Robertsonian translocations. Exp Cell Res 152:220–230; 1984.
3. Brady, K. P., Dushkin, H., Fornzler, D., Koike, T., Magner, F., Her, H., Gullans, S., Segre, G. V., Green, R. M., and Beier, D. R. A novel putative transporter maps to the osteosclerosis (oc) mutation and is not expressed in the oc mutant mouse. Genomics 56:254–261; 1999.
4. Courseaux, A., Szepetowski, P., Fernandes, M., Serizet, C., Kawaguchi, Y., Grosgeorge, J., Perucca-Lostanlen, D., Shows, T. B., Todd, J. A., Nowak, N. J., and Gaudray, P. Framework YAC contig anchored into a 3.2-Mb high-resolution physical map in proximal 11q13. Genomics 40:13–23; 1997.
5. Dickie, M. M. Private communication. Mouse News Letter 36:39; 1967.
6. European Backcross Collaborative Group. Towards high resolution maps of the mouse and human genomes: a facility for ordering markers to 0.1 cM resolution. Hum Mol Genet 3:621–627; 1994.
7. Ewing, B., Hillier, L., Wendl, M. C., and Green, P. Base-calling of automated sequencer traces using phred. I. Accuracy assessment. Genome Res 8:175–185; 1998.
8. Fernandes, M., Lespinasse, F., Rotomondo, F., Poirier, C., Guenet, J. L., Gaudray, P., and Carle, G. F. Comparative mapping of two adjacent regions of MMU19 with their human counterpart on HSA11q13. Cytogenet Cell Genet 81:237–246; 1998.
9. Fischer, A., Griscelli, C., Friedrich, W., Kubanek, B., Levinsky, R., Morgan, G., Vossen, J., Wagemaker, G., and Landais, P. Bone-marrow transplantation for immunodeficiencies and osteopetrosis: European survey, 1968–1985. Lancet 2:1080–1084; 1986.
10. Gerritsen, E. J., Vossen, J. M., van Loo, I. H., Hermans, J., Helfrich, M. H., Griscelli, C., and Fischer, A. Autosomal recessive osteopetrosis: variability of findings at diagnosis and during the natural course. Pediatrics 93:247–253; 1994.
11. Heaney, C., Shalev, H., Elbedour, K., Carmi, R., Staack, J. B., Sheffield, V. C., and Beier, D. R. Human autosomal recessive osteopetrosis maps to 11q13, a position predicted by comparative mapping of the murine osteosclerosis (oc) mutation. Hum Mol Genet 7:1407–1410; 1998.
12. Heinemann, T., Bulwin, G. C., Randall, J., Schnieders, B., Sandhoff, K., Volk, H. D., Milford, E., Gullans, S. R., and Utku, N. Genomic organization of the gene coding for TIRC7, a novel membrane protein essential for T cell activation. Genomics 57:398–406; 1999.
13. Hodgkinson, C. A., Moore, K. J., Nakayama, A., Steingrimsson, E., Copeland, N. G., Jenkins, N. A., and Arnheiter, H. Mutations at the mouse microphthalmia locus are associated with defects in a gene encoding a novel basic-helix-loop-helix-zipper protein. Cell 74:395–404; 1993.
14. Lane, P. W. Private communication. Mouse News Letter 52:37; 1975.
15. Li, Y. P., Chen, W., and Stashenko, P. Molecular cloning and characterization of a putative novel human osteoclast-specific 116-kDa vacuolar proton pump subunit. Biochem Biophys Res Commun 218:813–821; 1996.
16. Li, Y. P., Chen, W., and Stashenko, P. 21st Annual Meeting of the American Society for Bone and Mineral Research. St. Louis, MO, September 30 to October 4, 1999. Abstracts. J Bone Miner Res 14(Suppl. 1):S177; 1999.
17. Marks, S. C., Jr., Seifert, M. F., and Lane, P. W. Osteosclerosis, a recessive skeletal mutation on chromosome 19 in the mouse. J Hered 76:171–176; 1985.
18. Nakamura, I., Takahashi, N., Udagawa, N., Moriyama, Y., Kurokawa, T., Jimi, E., Sasaki, T., and Suda, T. Lack of vacuolar proton ATPase association with the cytoskeleton in osteoclasts of osteosclerotic (oc/oc) mice. FEBS Lett 401:207–212; 1997.
19. Schreiber, M., Poirier, C., Franchi, A., Kurzbauer, R., Guenet, J. L., Carle, G. F., and Wagner, E. F. Structure and chromosomal assignment of the mouse fra-1 gene, and its exclusion as a candidate gene for oc (osteosclerosis). Oncogene 15:1171–1178; 1997.
20. Stewart, C., Parente, F., Piehl, F., Farnebo, F., Quincey, D., Silins, G., Bergman, L., Carle, G. F., Lemmens, I., Grimmond, S., Xian, C. Z., Khodei, S., Teh, B. T., Lagercrantz, J., Siggers, P., Calender, A., Van de Vem, V., Kas, K., Weber, G., Hayward, N., Gaudray, P., and Larsson, C. Characterization of the mouse Men1 gene and its expression during development. Oncogene 17:2485–2493; 1998.
21. Szepetowski, P. and Gaudray, P. FCER1B, a candidate gene for atopy, is located in 11q13 between CD20 and TCN1. Genomics 19:399–400; 1994.
22. Yoshida, H., Hayashi, S., Kunisada, T., Ogawa, M., Nishikawa, S., Okamura, H., Sudo, T., and Shultz, L. D. The murine mutation osteopetrosis is in the coding region of the macrophage colony stimulating factor gene. Nature 345:442–444; 1990.

Date Received: November 1, 1999
Date Revised: December 6, 1999
Date Accepted: December 6, 1999